J Chem Crystallogr (2011) 41:87–97
DOI 10.1007/s10870-010-9931-3

REVIEW PAPER

Monomeric and Dimeric Erbium(III) Complexes: Crystal Structure and Photoluminescence Studies

Eny Kusrini · Muhammad I. Saleh · Anwar Usman

Received: 3 May 2010 / Accepted: 16 November 2010 / Published online: 17 December 2010

Abstract The crystal structure and photoluminescence (PL) studies of the monomeric and dimeric Er(III) complexes with two different chelating ligands (anthracene-9-carboxylic acid, 9-ACA; pentaethylene glycol, EO5; and picric acid, HPic) are reviewed. The Er(III) metal ion was coordinated to the attached ligands in eight- and nine-coordination number. The dimeric $[Er_2(9\text{-AC})_6(DMF)_2(H_2O)_2]$ complex shows the presence of deprotonated 9-AC anions with the negatively charged oxygen atoms bridged two Er(III) ions leads to a great coordinative flexibility via three possibilities of coordination modes, i.e. monodentate, chelation bidentate, chelating–bridging tridentate, where 9-AC = anthracene-9-carboxylate anion. The monomeric $[Er(Pic)_2(EO5)](Pic)$ complex displays the important flexible structure of the acyclic EO5 ligand and the role of Pic anions act as bidentate and monodentate chelations. The PL spectra of both Er(III) complexes show a broad band with the center peak position being dependent on the attached aromatic ligands. The heavier lanthanide complexes show the difference in structures, coordination geometry environment, and luminescence properties compared to the lighter lanthanide complexes. The energy transfer process in the complexes could be optimized with maximize the overlap between the emission spectrum of donor atom and absorption spectrum of acceptor atom.

Keywords Crystal structures · Dimeric · Erbium · Monomeric · Photoluminescence

E. Kusrini (✉)
Department of Chemical Engineering, Faculty of Engineering, Universitas Indonesia, 16424 Depok, Indonesia
e-mail: ekusrini@che.ui.ac.id

M. I. Saleh
School of Chemical Sciences, Universiti Sains Malaysia, 11800 Penang, Malaysia

A. Usman
Department of Applied Chemistry and Institute of Molecular Science, National Chiao Tung University, 30010 Hsinchu, Taiwan, Republic of China

Introduction

Since the Ln(III) complexes exhibit some interesting aesthetic structures and physical properties [1–5], there has been an increasing interest to design the functional Ln(III) complexes with some organic ligands from simple aromatic acids to bulky aromatic skeletons. Most of the studies on lanthanide complexes are intended to explore new crystal structure complexes as well as the physical properties to pursue a technique utilizing them as component in several important devices such as photoluminescence (PL), magnetisms, and electroluminescence (EL) [6–8]. Several Ln(III) ions are shown to luminescence in the visible or near-infrared spectral regions, upon irradiation with ultraviolet (UV) radiation. Interestingly, the emission is highly pure monochromatic, and the color of the emitted light is selective depending strongly on the Ln(III) ion, but not on the attached ligands. Furthermore, the Tm(III) ion emits exclusively blue light, Tb(III) in green light, Sm(III) in orange light and Eu(III) in red light. The Yb(III), Nd(III), Pr(III), Dy(III), Ho(III), and Er(III) ions are well-known for their near-infrared (NIR) emissions. The Gd(III) ion emits in the ultraviolet region, though it is highly quenched.

The Er(III) complexes have attracted much attentions due to its emission is applicable for planar optical amplifiers in telecommunication operating around 1500 nm as

well as for organic light emitting diode (OLED) [9–11]. The Er(III)-8-hydroxyquinolinate complexes is firstly applied as emitting center for OLED application in the infrared region (1540 nm). These particular complexes are often considered to have a 1:3 metal-to-ligand ratio, but the structural chemistry of their complexes is very complicated, like other lanthanide-quinolinates. The monomeric Er(II) complexes involving acac and phen (where aca = acetylacetone and Phen = 1,10-phenanthroline) have also been reported [12–14]. Both the $[Er(acac)_3]$ and $[Er(acac)_3(phen)]$ complexes have been used as emitting center to construct the near-infrared-emitting OLEDs [12–14]. The Er(III) complexes with some organic ligands have been structurally investigated, namely $[Er(Pic)_2(TTD)(H_2O)][Pic]\cdot CH_3CN$ [15], $[Er(Pic)_2(EO5)](Pic)$ [16], $[Er_2(9\text{-}AC)_6(DMF)_2(H_2O)_2]$ [17], $[Er(NCS)_3\{(py)_2C(OCH_3)(OH)_3\}]$ [18], $[Er(L1)_2(H_2O)_2]n[ClO_4]_{3n}\cdot nH_2O$ [19], $[Er(L2)_2(H_2O)]_n[ClO_4]_{3n}\cdot nH_2O$ [19], $[Er_2(Acc^6)_4(H_2O)_8](ClO_4)_6\cdot(H_2O)_{11}$ [20], $[(hexacyclen)Er(\mu\text{-}OH)_2Er(hexacyclen)]\cdot(CF_3SO_3)_4$ [21], $[Er_2(anth)_6(H_2O)_4]\cdot 2H_2O$ [22], and $[Er_2(NCS)_3\{(py)_2C(OCH_3)O\}_3(CH_3OH)]$ [20], where TTD = *N,N,N′,N′*-tetraphenyl 3,6,9-trioxa-undecanediamide, Pic = picrate anion, EO5 = pentaethylene glycol, 9-AC= anthracene-9-carboxylate anion, $(py)_2CO$ = di-2-pyridylketone, L1 = *N,N*-dicarboxymethyl-*N,N,N,N*-tetramethyl-1,3-propanediammonium, L2 = *N,N*-dicarboxy methyl-*N,N,N,N*-tetramethyl-1,4-butanediammonium, Acc^6 = 1-amino cyclohexane-1-carboxylicacid, hexacyclen = 1,4,7,10,13,16 hexaazacyclooctadecane and anth = anthranilate. The coordination number of the Er(III) complexes is in the range of 8–9 [15–22].

In our previous reports, we have studied that the Er(III) ion makes complexes either with the anthracene-9-carboxylic acid (9-ACA) ligand in the mixture of H_2O:DMF solution or with the non-aromatic pentaethylene glycol (EO5) in the presence of picric acid (HPic) [16, 17], which allow us to explore further the effect of the bulky aromatic ring skeleton in the formation of complex. In this paper, we would like to review our work on one-pot syntheses, crystal structures, and photoluminescence (PL) properties of monomeric and dimeric Er(III) complexes having 9-ACA, HPic, and EO5 as chelating ligands. The crystal structures and PL properties of other Ln(III) complexes are also discussed to observe the effect of lanthanide ion in the coordination environment and luminescence properties. The participation of the 4f orbital in bonding is small with overlap values in general smaller than 5% [23, 24]. This is due to the shielding of the 4f orbitals by the $5s^2$ and $5p^6$ filled sub-shells [25], thus the luminescence properties of Ln(III) ions in the complexes are essentially ascribed to those of lanthanide free ions [26].

Experimental

Materials

All chemicals and solvents were of analytical grade and used without further purification. Pentaethylene glycol (EO5, $C_{10}H_{22}O_6$, ≥97% purity) was purchased from Fluka (Buchs, Switzerland). HPic ($(NO_2)_3C_6H_2OH$, >98% purity) was purchased from BDH (Poole, England). 9-ACA ($C_{15}H_{10}O_2$, 98% purity) was purchased from Merck (Germany). $Er(NO_3)_3\cdot 5H_2O$ (99.9% purity) was purchased from Aldrich (Wisconsin, USA). Er_2O_3 (99.9% purity) was purchased from Sigma–Aldrich (Steinheim, Germany). Hydrochloric acid 37% was obtained from Fisher Chemicals (Leicestershire, England).

Synthesis of Erbium Complexes

The $[Er_2(9\text{-}AC)_6(DMF)_2(H_2O)_2]$ and $[Er(Pic)_2(EO5)](Pic)]$ complexes were synthesized from the reactions of erbium salt with different chelating ligands, i.e. 9-ACA in the mixture of H_2O:DMF solution and EO5 in the presence of HPic, by using a one-pot synthesis method as previously reported by Kusrini and coworkers [16, 17].

Preparation of $ErCl_3\cdot 6H_2O$ and the Sodium Salt of ACA Ligand

$ErCl_3\cdot 6H_2O$ was synthesized following the method was reported by Yang et al. [27]. The procedure was described as follow: Erbium oxide (Er_2O_3) (191.3 mg, 0.5 mmol) was added into an aqueous solution 6 mL of hydrochloride acid 37% by volume ratio of 1:5 (v/v). The mixture was heated at 60–70 °C in waterbath until a clear solution was obtained. The solution was left to stand for several days at room temperature and the pink solid were collected after several days. $ErCl_3\cdot 6H_2O$ was characterized by termogravimetric analysis (TGA) and confirmed that the content of water molecules is hexahydrate.

Briefly, first, the sodium salt of 9-ACA ligand was synthesized by adding equivalent mole in 1:1 ratio of 9-ACA (444.5 mg, 2 mmol) and NaOH (80 mg, 2 mmol) in distilled water. Afterwards, the aqueous suspensions of acid and NaOH were continuously heated at 70 °C in waterbath and stirred vigorously for 30 min. The yellow solution was evaporated until dryness. The sample was kept in desiccator for further analysis.

Preparation of the $[Er_2(9\text{-}AC)_6(DMF)_2(H_2O)_2]$ Complex

NaOH (20.0 g, 0.5 mol) was dissolved in distilled water at room temperature. The colorless solution was diluted to

100 mL using volumetric flask of 100 mL capacity. The 5 M NaOH solution was stored in polypropylene bottles.

To sodium salt of 9-ACA (732.7 mg, 3 mmol) and $ErCl_3 \cdot 6H_2O$ (381.6 mg, 1 mmol) was dissolved in 20 mL distilled water followed by the addition of 5 mL DMF with slowly constant stirring. Adjust the pH value of the mixture solution to 6.0 by adding 5 M NaOH solution (0.5 mol of NaOH is diluted in 100 mL water). After a clear solution was obtained, the mixture was heated for 20 min in waterbath at temperature of 70 °C. Immidiately, the mixture solution was filtered using ordinary grade filter paper. Afterwards, the mixture was left to stand for several days to allow the evaporation at room temperature and the yellowish orange crystals were obtained. Yield: 46.2%. Anal. Calc. for $C_{96}H_{72}Er_2N_2O_{16}$: C, 62.40; H, 4.01; N, 1.52. Found: C, 62.45; H, 3.19; N, 1.46%. Significant peaks in IR (KBr) cm^{-1}: ν(OH) 3418, ν(C=O) 1661, ν_a(COO) 1552, ν_s(COO) 1389, ν_a(C–N) 1114, and ν_s(C–N) 853 [17].

Preparation of the [Er(Pic)$_2$(EO5)](Pic) Complex

A mixture of EO5 (600 mg, 2.52 mmol), HPic (910 mg, 3.97 mmol), and $[Er(NO_3)_3 \cdot 6H_2O]$ (434 mg, 1 mmol) was dissolved in 20 mL acetonitrile:methanol (3:1, v/v). The solution was stirred for 5 min. The solution was left to stand for several days at room temperature and single crystals were collected. Yield: 60%. Anal. Calc. for $C_{28}H_{28}N_9O_{28}Er$: C, 30.74; H, 2.47; N, 11.53. Found: C, 30.84; H, 2.61; N, 10.97%. Significant peaks in IR (KBr) cm^{-1}: ν(OH) 3414, ν(C–H) Ar 3084, ν(C–H) methylene 2959 m, $\nu_{as}(NO_2)$ 1561; 1535, $\nu_s(NO_2)$ 1370; 1336, ν(C–C) 1278, δ(C–O) Ar 1164, ν(C–O) 1082, ν(C–N) 938; 790 [16].

Physical Measurements

The elemental analyses were determined by using a Perkin-Elmer 2400II elemental analyzer. IR spectra were recorded on a Perkin-Elmer 2000 FTIR spectrophotometer in the region of 4000–400 cm^{-1} by using the conventional KBr pellet method for solid samples. For liquid sample, e.g. DMF, a thin layer of sample was applied to the surface of a KRS-5 (Thallium bromoiodide). Thermogravimetric analyses (TGA) were performed on a Perkin-Elmer TGA-7 series thermal analyzer under a nitrogen atmosphere, with a heating rate of 20 °C/min. The UV–Vis spectra in the solid state were determined by using a Perkin-Elmer Lambda 35 UV–Vis spectrophotometer.

Photoluminescence (PL) measurements were made at room temperature by using a Jobin–Yvon HR800UV system. The data were collected and processed with Labspec Version 4 software. An HeCd laser was used for excitation at 325 nm, and the emission spectra were scanned from 330 to 1000 nm.

X-Ray Crystallographic Study

X-ray diffraction data was collected from single crystal by using a Bruker APEX2 area-detector diffractometer with a graphite monochromated Mo Kα radiation source and a detector distance of 5 cm. Data were processed using APEX2 software [28]. The collected data were reduced by using the SAINT program and the empirical absorption corrections were applied with the SADABS program [28]. The structures were solved by direct methods and refined by least-squares method on F^2_{obs} using the SHELXTL program [29]. All non-hydrogen atoms were refined anisotropically. Hydrogen atoms were located from different Fourier maps and were isotropically refined. The final refinement converged well. Data for publication were prepared with SHELXTL [29] and PLATON [30]. Crystal data and structure refinement for the Er(III) complexes are listed in Table 1. Selected bond lengths of the Er(III) complexes are summarized in Table 2.

Results and Discussion

Crystal Structures

Considering that the coordination site of 9-ACA and benzoic acid are similar, because both organic ligands have one carboxylic group at the same position in different plane on the bulk of the aromatic skeleton of the 9-ACA ligand. The complexes of $[Er_2(9\text{-}AC)_6(DMF)_2(H_2O)_2]$, where 9-AC stand for anthracene-9-carboxylate anion, crystallizes in monoclinic system with space group $P2_1/c$. The Er(III) center ion is coordinated to the ligands via Er–O bonds with a eight coordination number. The structure of the complex lies on mirror plane passing through the C7, C14; C22, C29; C37, and C44 atoms, making the complex in a dimeric unit or a dinuclear structure of two $[Er(9\text{-}AC)_3(DMF)(H_2O)]$ moieties. It is noted that the six 9-AC anions in the dimeric complex are linked symmetrically to the two Er(III) ions, and all the 9-AC anions are in the deprotonated form and adopt three kinds of coordination modes, i.e. monodentate, chelation bidentate, and chelation–bridging tridentate (Fig. 1).

The nonbonded Er(III)–Er(III) distance in the centrosymmteric structure is the same as 4.015 Å. The two Er(III) ions are bridged via two carboxylato groups from the 9-AC anions, forming an inversion symmetric square plane of Er1–O1–Er1A–O1A four membered-ring. In the dimeric complex, the chelating bidentate (*O*,*O*), chelating–bridging tridentate (*O*,*O*,*O*) and monodentate of 9-AC anions are observed. The one DMF and one water molecules are also incorporated in the dimeric complex. The 9-AC anions display the similar coordination mode of

Table 1 Crystal data and structures refinement for the monomeric and dimeric Er(III) complexes

Parameter	$Er_2(9\text{-AC})_6(DMF)_2(H_2O)_2$	$[Er(Pic)_2(EO5)](Pic)$
Formula	$C_{96}H_{72}Er_2N_2O_{16}$	$C_{28}H_{28}N_9O_{28}Er$
Molecular weight	1844.08	1089.85
Temperature (K)	100(0)	293(2)
Crystal system, space group	Monoclinic, $P2_1/c$	Monoclinic, $P2_1/c$
Unit cell dimensions		
a (Å)	13.9387(4)	18.707(8)
b (Å)	13.6552(4)	8.980(4)
c (Å)	20.9439(6)	24.077(1)
$\alpha = \gamma$ (°)	90	90
β (°)	101.2470(10)	109.252(1)
Volume ($Å^3$)	3909.8(2)	3818.5(3)
Z	2	4
Dx (g/cm^3)	1.566	1.896
μ (mm^{-1})	2.205	2.314
F(000)	1852	2172
Crystal size (mm)	0.36 × 0.24 × 0.23	0.50 × 0.34 × 0.34
θ (°)	2.11–32.50	2.41–28.29
h, k, l	−18/21, −20/20, −31/31	−24/21, −11/11, −20/31
Reflections collected/unique	41043/13780	22884/9329
[R(int)]	0.0367	0.021
Completeness to theta (%)	97.4	98.6
Refinement method	Full-matrix least-squares on F^2	Full-matrix least-squares on F^2
Data/restraints/parameters	13780/2/531	9329/0/586
Goodness-of-fit on F^2	1.032	1.071
Final R indices [$I > 2\sigma(I)$]	R1 = 0.0282, wR2 = 0.0660	R1 = 0.0322, wR2 = 0.081
R indices (all data)	R1 = 0.0345, wR2 = 0.0695	R1 = 0.040, wR2 = 0.086
$\Delta\rho$max, $\Delta\rho$min ($e/Å^3$)	1.383, −0.684	1.384, −0.850

chelating–bridging tridentate to that in the $[Ag_6(9\text{-AC})_6(dmp)_2]$ complex, where dmp stands for 2,6-dimethylpyridine [31] and the steric anthracene rings of the 9-AC anions play important roles in the formation of dimeric complex. The three anthracene cores of the 9-AC anions are planar and forming a 14-membered ring, as expected for aromatic ring, and it is similar with the free 9-ACA ligand [32].

The monomeric complex of $[Er(Pic)_2(EO_5)](Pic)$ contains two crystallographically independent $[Er(Pic)_2(EO5)]^+$ and a $[Pic]^-$ anion in the asymmetric unit. The Pic anion is the negatively charged at the phenolic oxygen and the Er(III) ion interacts with the Pic by ion–ion interaction. The distance between the phenolic and nitro oxygen atoms of about 2.7 Å that are coordinated with the Er(III) ion, leading to an effective bidentate mode due to the effect from both charge and dipole binding ability [33]. Thus, the Er(III) ion is coordinated to nine donor oxygen atoms, i.e. six oxygen atoms from the EO5 ligand in hexadentate mode and the other three from bidentate and monodentate Pic anions (Fig. 2). The acyclic EO5 ligand was coordinated to the lanthanide metal ion in a pseudo-cyclic conformation [1–8]. The positively charged complex is balanced by one Pic anion. The monomeric $[Er(Pic)_2(EO5)](Pic)$ complex is isostructural with several complexes of $[Ln(Pic)_2(EO5)](Pic)$, where the Ln(III) ions are La–Ho and Y [1–5, 16]. The Ln(III) ions control the geometry of the inner coordination spheres in the Ln–Pic complexes [34]. In all of the $[Ln(Pic)_2(EO5)](Pic)$ complexes, the aromatic ring of the two coordinated Pic anions are almost perpendicular with the structures of the cation. The presence of the Pic anion can prevent the water molecules involved in the inner coordination sphere [34].

The coordination geometries of the two Er(III) ions in the dimeric $[Er(9\text{-AC})_3(DMF)(H_2O)]$ complex adopt a triangular dodecahedron with symmetry D_{2d} (Fig. 3a). The dihedral angle between the plane of the carboxyl group from the chelating–bridging tridentate 9-AC anion and the best-fit core anthracene plane is the smallest, due to the balancing position between two $[Er(9\text{-AC})_3(DMF)(H_2O)]$ moieties in a propeller-arrangement. The DMF molecule has one C=O group involved in the inner coordination sphere of the complex. In the monomeric $[Er(Pic)_2(EO_5)](Pic)$ complex, the coordination geometries around

Table 2 Selected bond length in the monomeric and dimeric Er(III) complexes

Bond	Length (Å)
$Er_2(9\text{-AC})_6(DMF)_2(H_2O)_2$	
Er1–O7	2.248(1)
Er1–O5	2.256(1)
Er1–OW1	2.296(1)
Er1–O1	2.495(1)
Er1–O4	2.386(1)
Er1–O3	2.399(2)
Er1–O2	2.409(1)
Er1A–O1	2.319(1)
$[Er(Pic)_2(EO5)](Pic)$	
Er1–O1	2.419(2)
Er1–O2	2.507(3)
Er1–O3	2.478(3)
Er1–O4	2.424(3)
Er1–O5	2.510(2)
Er1–O6	2.450(2)
Er1–O7	2.270(2)
Er1–O14	2.268(2)
Er1–O8	2.445(3)

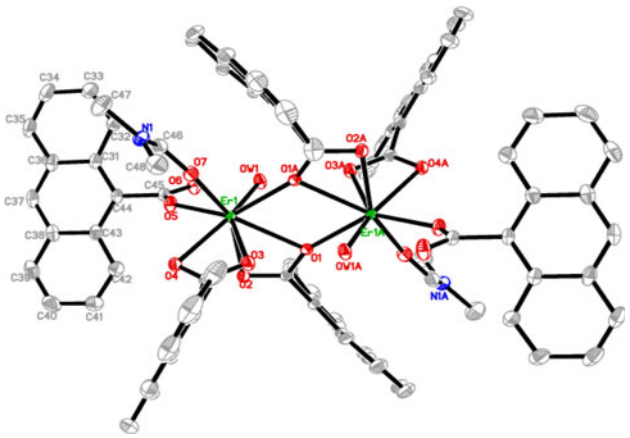

Fig. 1 Molecular structure of the dimeric $[Er_2(9\text{-AC})_6(DMF)_2(H_2O)_2]$ complex with thermal ellipsoids 50% probability. The hydrogen atoms are omitted for clarity

the Er1 atom is a distorted tricapped trigonal prismatic (TTP) geometry with the three oxygen atoms at the peak of the capping position of the three square planes, namely O2–O14–O6–O8, O4–O14–O2–O7, and O4–O6–O8–O7. The Er(III) ion lies on the center of this trigonal plane (Fig. 3b). The distorted TTP geometry for the monomeric complex is caused by the edge distances of O6–O4 (3.837 Å) and O8–O7 (2.680 Å) that are less coplanar and are not equivalent. Beside, the edge distances of O6–O1 (2.913 Å) and O6–O8 (2.971 Å) as well as in the edge distances of O3–O4 (2.601 Å), O5–O4 (2.566 Å) and

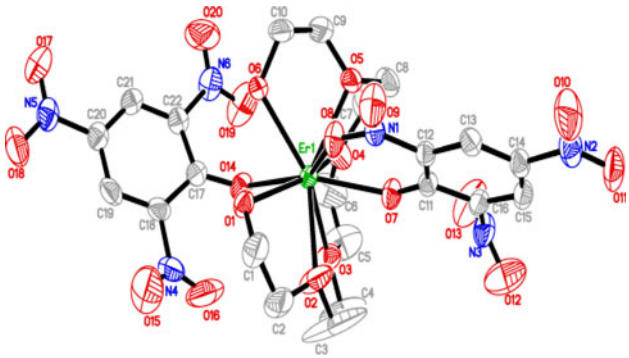

Fig. 2 Molecular structure of the monomeric $[Er(Pic)_2(EO5)](Pic)$ complex with thermal ellipsoids 50% probability. The hydrogen atoms and a counter-anion of Pic are omitted for clarity

O8–O2 (3.472 Å) are not parallel. Thus, the coordination geometry environment around the Er1 atom in the monomeric complex is not a capped square antiprism geometry. This because of the O1–O2–O3–O14 atoms are not coplanar due to the edge distance of O2–O14 towards the O1–O2–O3–O14 square is not planar.

The Er–O bond lengths in the $[Er_2(9\text{-AC})_6(DMF)_2(H_2O)_2]$ lie between 2.248(1) and 2.495(1) Å, including the chelating–bridging tridentate, bidentate, and monodentate bonds to the 9-AC anion and to DMF molecule. In the dimeric complex, the coordinated water molecule was positioned between two carboxyl groups. In the monomeric complex of $[Er(Pic)_2(EO5)](Pic)$, the Er–O bond lengths of oxygen ether are longer than the Er–O of oxygen phenol (2.269(2) Å). This short of bond length is caused by the higher electron density of the phenolic oxygen of the Pic anion [1–8]. The Er–O bond length of oxygen nitro group is shorter than those found in the lighter lanthanide–picrate complexes [1–8]. This bond length is influenced by the free position of the *ortho*-nitro oxygen atoms before this oxygen is coordinated with the metal ion. The O–Er–O bond angles between the adjacent oxygen atoms in the inner coordination sphere are approximately 60°. These angles are similar to that in other complexes of $[Ln(Pic)_2(EO5)](Pic)$ [1–5, 16].

The whole structure of the dimeric complex of $[Er_2(9\text{-AC})_6(DMF)_2(H_2O)_2]$ resembles a propeller-like construction with the 9-AC anions acting as a fan. We note that in the dimeric complex, one of the oxygen atom of the monodentate 9-AC anion does not participate in the coordination to the Er(III) ions, but this atom is important for stabilizing the structure by a strong intramolecular hydrogen bonding (O_W–H_W···O) (see Fig. 4). The free steric anthracene rings and carboxyl group allow the 9-AC anions to form a variety of coordination modes. Five intramolecular O–H···O and C–H···O hydrogen bonds, beside numerous intermolecular C–H···π supramolecular interactions are observed in the crystal packing help to stabilize of

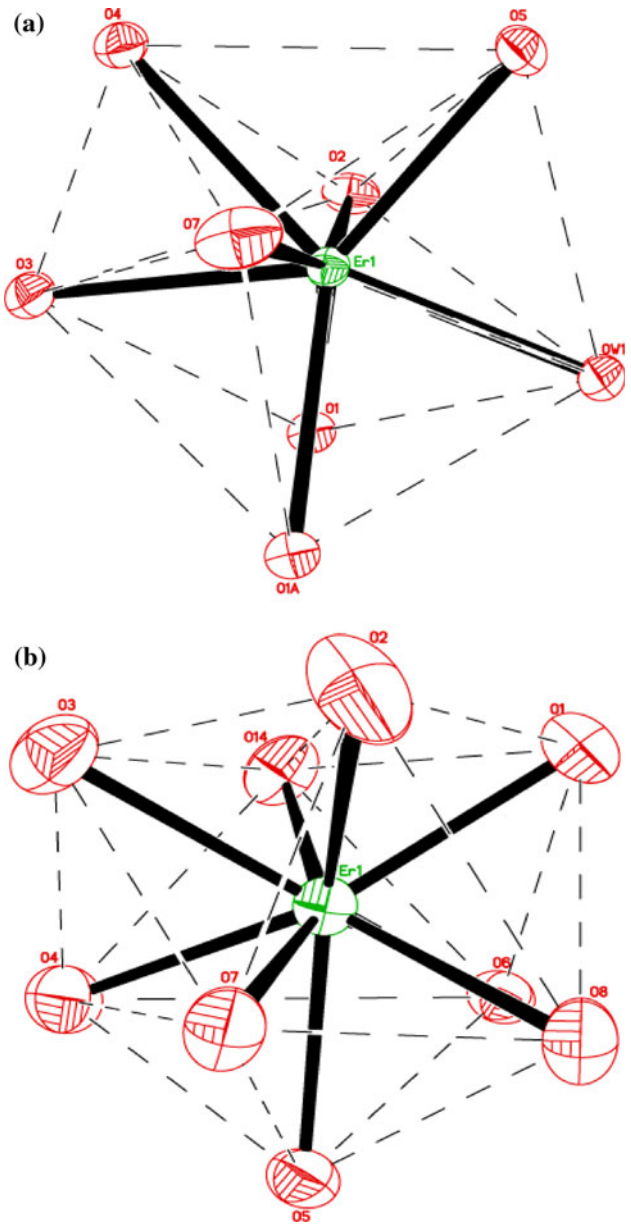

Fig. 3 The coordination geometry environment around the Er(III) ion as a triangular dodecahedron (**a**) and tricapped trigonal prismatic (**b**)

complex. Several edge-to-face and weak hydrogen bond interactions are liable for characteristic herring bone packing in the crystal structure of dimeric complex.

In the monomeric $[Er(Pic)_2(EO5)](Pic)$ complex, the geometric conformational pattern in the EO5 ligand is g^+ g^- g^+ g^- g^- with following average O–C–C–O torsion angles of 37.3(8)°. The similar pattern is observed in the $[Tb(Pic)_2(EO5)](Pic)$ and $[Y(Pic)_2(EO5)](Pic)$ complexes. The complex shows one-dimensional (1D) architecture in the [001] direction that is interconnected by intra- and intermolecular O–H···O and C–H···O hydrogen bonds (Fig. 5). The terminal alcoholic group offers the possibility in the formation of strong and weak hydrogen bonds to attain high stability of the complex so that resulting in the formation of two bifurcated hydrogen bonds. The $[Er(Pic)_2(EO5)]^+$ cation and the Pic counter anion have contributed to involve in the formaton of intermolecular weak hydrogen bonds and π–π interactions. Interestingly, the relative orientation of the two adjacent aromatic rings of the Pic anion is determined by the electrostatic repulsions between the two negatively charged π-systems. It is interesting to note that especially for the acyclic EO5 ligand, the two terminal alcohol groups and the aliphatic group may quench the Er(III) luminescence, because of highly efficient non-radiative deactivations of the O–H and C–H groups, leading to their vibrational couplings with the vibrational state of the O–H and C–H oscillator and low luminescence quantum yield [35]. The electron-withdrawing ability of phenolic and nitro groups in the Pic anions is also considered to affect the distribution of π-electronic density. Nevertheless, from both Er(III) complexes, we can draw a conclusion that the unique coordination of Er(III) complex architectures can be easily constructed by introducing potential chelating ligands having either steric hindrance of the bulky aromatic rings or nonaromatic compounds. The ability of the 9-AC, EO5, and Pic ligands to satisfy the coordination requirements of the central Er(III) with a high coordination number is also an important criterion in the design of supramolecular photonic devices. Thus, this provides further studies on their physical properties and applications (Figs. 6, 7).

Photoluminescence of Er(III) Complexes

Several Ln(III) ions has shown to luminescence in the visible or near-infrared (NIR) spectral regions upon irradiation with ultraviolet radiation. The color of the emitted photoluminescence light depends strongly on the Ln(III) ion, and it is attributed to the triplet-to-singlet emission or from a spin-forbidden transition. In the case of the Ln(III) ion, the emission is due to transitions inside the 4f shell, i.e. intraconfigurational 4f → 4f transitions. Generally, since the 4f shell is well shielded from other closest shells, the electronic 4f–4f intraconfigurations of the Ln(III) ions is only perturbed in a very limited extent by the surrounding ligands. This shielding transition is responsible for the specific properties and narrow-band emission of the PL of the Ln(III) complexes.

The PL spectrum of the monomeric $[Er(Pic)_2(EO5)](Pic)$ complex shows typically a broad band with the center peak at 535 nm based on D2 filter measurement (Fig. 6). Similar broad spectrum is observed for the dimeric $[Er_2(9\text{-AC})_6(DMF)_2(H_2O)_2]$ complex (Fig. 7). It is known that the lowest excited resonance level $^4I_{13/2}$ of Er(III) is 6506 cm^{-1} [36]. The less featured emission is likely due to

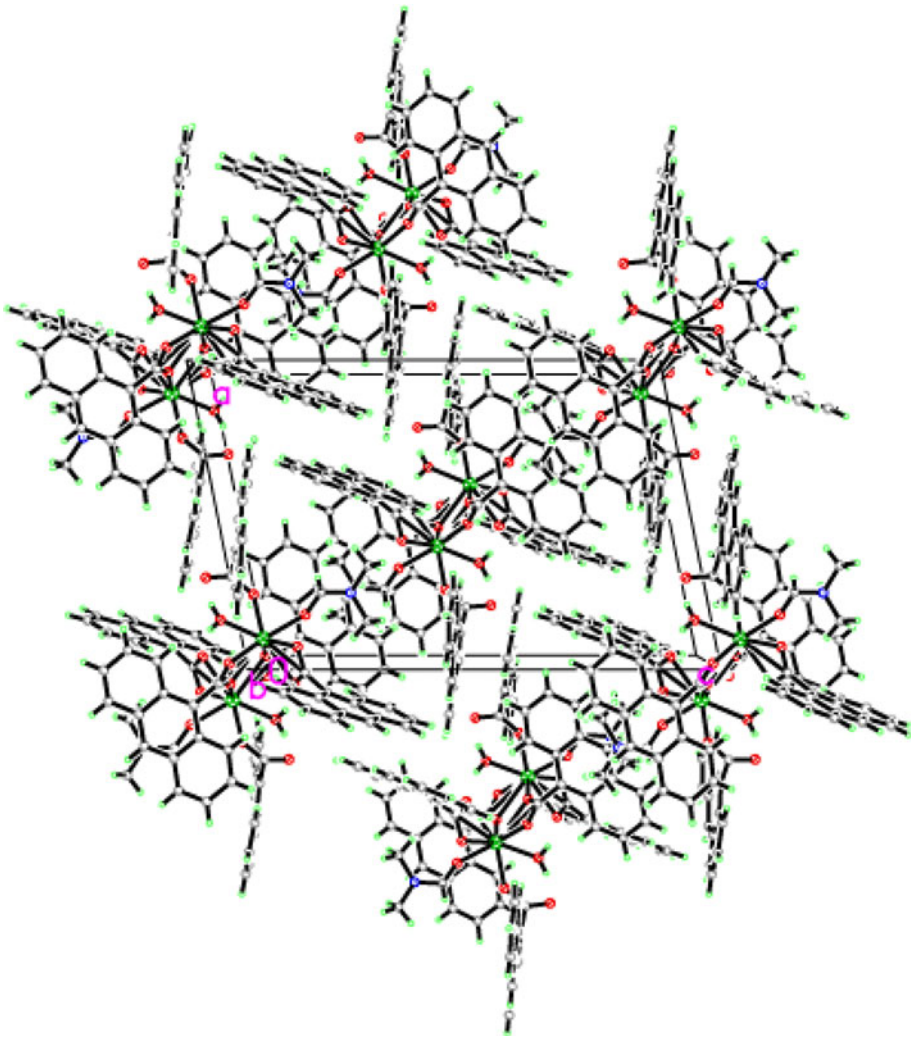

Fig. 4 A propeller-arrangement of $[Er_2(9\text{-AC})_6(DMF)_2(H_2O)_2]$ with the 9-AC anions act as a fan in unit cell viewed along *b*-axis

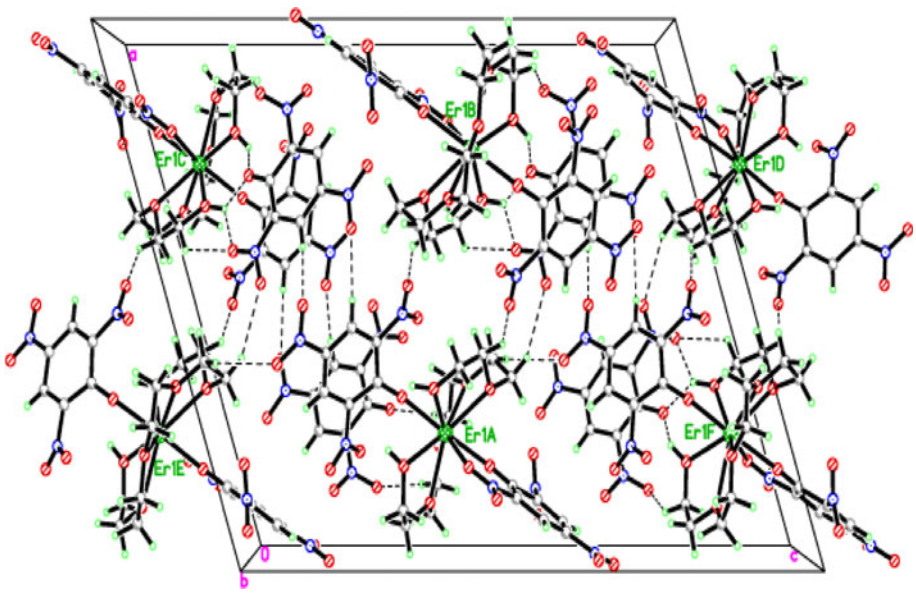

Fig. 5 The crystal packing of monomeric $[Er(Pic)_2(EO5)](Pic)$ complex is viewed along b-axis. The *dashed lines* indicate the C–H···O and O–H···O hydrogen bonds

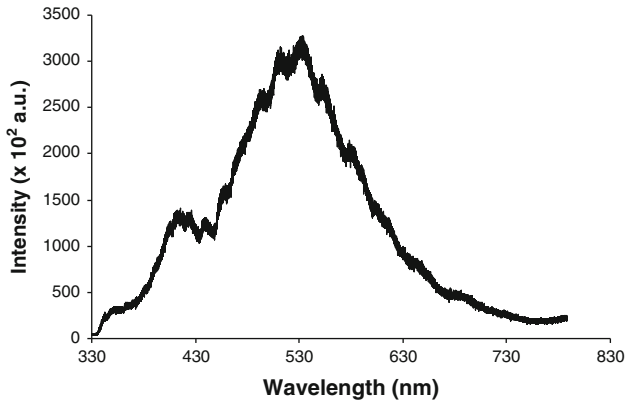

Fig. 6 The photoluminescence spectrum of the monomeric $[Er(Pic)_2(EO5)](Pic)$ complex in the solid state

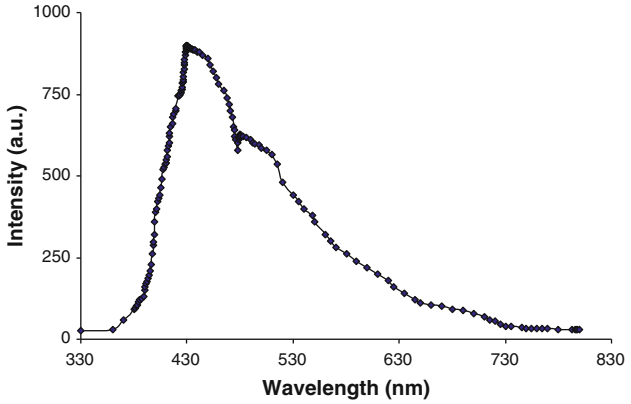

Fig. 7 The photoluminescence spectrum of the dimeric $[Er_2(9\text{-}AC)_6(DMF)_2(H_2O)_2]$ complex in the solid state

the emission of the ligands, and indicates that the emission Er(III) ion is not observed. Similar phenomena is observed for $[Ln(Pic)_2(EO5)](Pic)$, where Ln = Nd, Gd, Ho, Tm, and Y, and it is suggested that the transition of those Ln(III) ions may locate outside the spectral region observed due to the stability of the half-filled $4f^7$ shell configuration in the Ln(III) ions. This is in contrast to the other complexes of $[Ln(Pic)_2(EO5)](Pic)$ where the Ln(III) ion is Eu, Tb or Yb, which shows the typical 4f–4f intra-configuration transition emissions.

In order to figure out that PL spectrum of the monomeric $[Er(Pic)_2(EO5)](Pic)$ complex, the PL spectra of HPic and the free EO5 molecules were also investigated. We expect the HPic molecule to emit in the green region. The HPic molecule had a broad emission band with the center peak at 537 nm (18622 cm^{-1}) based on the D2 measurement. A broad emission peaks with the highest intensity at 492.8 nm (20292 cm^{-1}) is observed for the PL spectrum of the EO5 ligand. Since the EO5 molecule is the aliphatic chain structure with sigma-bonded and no aromatic compound, so that no emission peak of the acyclic EO5 ligand could be observed. In addition to that, the emission peaks for aliphatic chain appeared because of some impurities that probably present in the EO5 molecule. We noted that the triplet energy level of a conjugated system in the HPic molecule would most certainly be located at a lower energetic position than that of a sigma-bonded polyether molecule [7].

The free 9-ACA ligand has broad peak from 450 to 700 nm with the center peak at 530 nm in greenish blue luminescence. This indicates clearly that the PL spectra of both complexes are due to the emission from of the surrounding ligands. In the monomeric complex, the excitation energy in the short-wavelength of Er(III) transitions and the excited state of the Pic anions are transferred to the nitro group through $n \rightarrow \pi^*$ transition with an admixture of intra-ligand charge transfer (ILCT) being in the region of 350–425 nm. The excitation energy is dissipated in the lattice and further transferred to the lowest excited ligand triplet level, generating ligand fluorescence and Er(III) luminescence.

Similar phenomena are observed for the dimeric complex. The unfavorable energy transfer from the ligands to the Er(III) ion is clearly understood when we refer to the lowest triplet state energy level of the 9-ACA ligand, which is 18,868 cm^{-1} (530 nm). This energy level is much higher than the lowest excited resonance level of Er(III) ion [26]. The lowest triplet state of the ligand should be nearly equal to or at above a resonance level of the central ion concerned. In the $[Er(Pic)_2(EO5)](Pic)$ complex, the lowest triplet state energy level of the EO5 ligand should also be considered, but it is 20292 cm^{-1}, which is again much higher to the lowest excited resonance level of Er(III) [6506 cm^{-1}]. Thus, there is no intramolecular energy transfer from the excited chelating molecules to the central ion resulting in the increasing emission intensity of the Er(III) complexes. This is in contrast to when the Er(III) ion is replaced by the Eu(III) or Tb(III) ions, the lowest triplet state of the HPic and EO5 ligands are close to their lowest resonance levels of Eu(III) at $^5D_0$ (17300 cm^{-1}) and Tb(III) at $^5D_4$ (20500 cm^{-1}). Thus, the triplet state energy level of ligand is primarily transferred from ligand to the Ln(III) for Ln = Eu and Tb. In the $[Eu(Pic)_2(EO5)](Pic)$ complex shows the 4f–4f intraconfigurational with emission peaks that assigned for $^5D_0 \rightarrow {}^7F_{0-4}$ and $^5D_1 \rightarrow {}^7F_{2,4}$ transitions are observed in the red spectral region. While in the $[Tb(Pic)_2(EO5)](Pic)$ complex displays the emission peaks that related to the 4f–4f intraconfigurational with $^5D_4 \rightarrow {}^7F_J$ (J = 0, 2, 3, 4, 5, 6) transitions are shown in the green spectral region [16].

Since the energy gap between the lowest triplet state and the lowest excited resonance level of the Er(III) ion is very large; thus, the energy could not be transferred from the ligand to the Er(III) ion. Thus, the broad emission spectrum of the complexes composed of a broad band with the center

peak at 430 nm in $[Er_2(9\text{-}AC)_6(DMF)_2(H_2O)_2]$ or 537 nm in $[Er(Pic)_2(EO5)](Pic)$ due to the emission of intraligand $\pi^* \rightarrow \pi$ transition from the 9-AC and Pic anions, respectively, and a shoulder peak originating from the 4f–4f emission transition of the Er(III) ion. We think the PL spectrum of the monomeric complex is much more likely that it's due to the HPic molecule. The PL spectra of both complexes should exhibit the characteristic emission of the Er(III) ion, which is centered at 480 nm and attributed to its $^4F_{7/2} \rightarrow {}^4I_{15/2}$ transition upon excitation of the 9-AC and Pic anions with UV light excitation. This has been confirmed by UV–Vis measurement, where the dimeric $[Er_2(9\text{-}AC)_6(DMF)_2(H_2O)_2]$ complex had a 100 nm blue-shifted emission relative to the free 9-ACA ligand. The coordination with the Er(III) ions and the emission of ligand-to-metal charge transfer (LMCT) are considered to affect the emission spectral shift. It is noted that the NIR emission of Er(III) ion is also of interest, although such an emission can be strongly lowered by vibrational deactivation, especially, in the presence of the coordinated water molecules and a high-energy oscillations of O–H and C–H bonds from the polyether molecule. These oscillations will be able to quench the excited states of the metal ions nonradiatively, leading to decrease in the luminescence intensities and shorter excited state lifetime.

Comparison with Other Ln(III) Complexes

The crystal structures and PL properties of other Ln(III) complexes are also reviewed for comparison purposes. It is interesting to know the luminescence properties of other Ln(III) complexes with the same ligands to the $[Er(Pic)_2(EO5)](Pic)$ complex. For the EO5 ligand, the crystal structure of the $[Tb(NO_3)_2(EO5)](NO_3)$ complex has been reported by Rogers et al. [37] and we have also studied its PL in various solvents at an excitation wavelength of 275 nm. The crystal solid of the $[Tb(Pic)_2(EO5)](Pic)$ complex in DMSO solution had three peaks at 488, 549, and 615 nm. The $[Ln(Pic)_2(EO5)](Pic)$ complexes for Ln = Yb or Tb, have the lowest excited resonance level of the Ln(III) ion similar to the $[Er(Pic)_2(EO5)](Pic)$ complex. Thus, the excited energy could not be transferred from the lowest triplet state to the Yb(III) ion. The broad line of its PL is due to structural disorder and coordinated terminal alcohol groups.

The fluorescence spectrum of the $[Tb(NO_3)_2(EO5)](NO_3)$ complex in solution shows the typical spectral features of the Tb(III) ion, i.e. $^5D_4 \rightarrow {}^7F_6$ (491 nm), $^5D_4 \rightarrow {}^7F_5$ (541 nm), $^5D_4 \rightarrow {}^7F_4$ (585 nm), and $^5D_4 \rightarrow {}^7F_3$ (617 nm) transitions. The strong line emissions may be resulted by the different symmetry of Tb(III) in the complex, the rigid structure of the complex formed by two nitrate anions and one of the EO5 ligand, or the equivalent distances between the Tb(III) ion and the donor oxygen atoms. Vibrational quenching of the emission of the complex was thought to occur through a high energy oscillation to the solvent molecule [35, 38, 39]. An interesting comparison to the quenching effect is shown by the related complexes of $[Eu(Pic)_2(EO5)](Pic)$ and $[Tb(Pic)_2(EO5)](Pic)$, where the Pic anion acts as a quencher due to the nitro withdrawing groups, which was clearly observed in both solution and the solid state. Thus, this complex is not suitable for organic light emitting diode devices because of its ionic character and low volatility.

For the Ln(III) complexes, the quantum yield depends on the excited state of the ligand or metal ions, because the sensitization of the Ln(III) ion can occur by some energy migration paths. The efficiency of the energy transfer process depends on the particular energy transition levels. In this review, the energy transfer process is not efficient and incomplete. Therefore, an investigation and searching on a sensitizer is very important, expecting to find doped organic compounds that can perform the excitation energy transfer upon excitation via the sensitizer as an antenna to enhance the luminescence intensity.

In the Er(III)-8-hydroxyquinolinate complexes with a sensitizer like an ormosils at different composition in order to have the near-infrared luminescence of the complexes in a sol–gel matrix have been reported [40]. Most of the sensitizers of the Ln(III) ions in sol–gel materials are organic ligands. Nevertheless, the inorganic ligand as a sensitizer is probably to use such as lanthanide containing polyoxometalates in sol–gel derived materials. The use of organic ligands that possess a strong light absorption is also interesting in the Ln(III) complexes and is an advantage for sensitizing the luminescence of Ln(III) ions by the antenna effect. Combinations of the aromatic and aliphatic substituents such as in the monomeric $[Er(Pic)_2(EO5)](Pic)$ complex is expected to give the Er(III) complex with a more intense luminescence, if the excitation and energy transfer process is efficient. Similar observation has been made in the Eu(III) with β-diketones complexes. In these systems, the combinations results are in more efficient energy transfer process from the ligand to the Eu(III) ion. This is due to the increase in anisotropy around the Eu(III) ion [41]. We can optimize the energy transfer process and increase the quantum yield as well as enhance the luminescence intensity through maximize the overlap between the emission spectrum of donor atom and absorption spectrum of acceptor atom [42]. Three factors to enhance the luminescent intensity for the Ln(III) complexes and also as a sensitizers, i.e. (i) saturated coordination sphere, (ii) rigid and protective enviroment, and (iii) adequate electronic orbital [42].

Conclusion

This review shows that our research in the field of lanthanide-based photoluminescence materials is promising in finding some new Er(III) complexes with aromatic ligands. Moreover, the synthetic method is a simple one-pot reaction method, giving high quality crystals of the complexes. This should be accounted as one of the research works on Er(III), which is gradually increased and shifted toward more complex systems. The dimeric $[Er_2(9\text{-AC})_6(DMF)_2(H_2O)_2]$ complex is the first structurally investigated in our laboratory. The 9-AC anions with the negatively charged oxygen atoms bridged two Er(III) ions leads to a great coordinative flexibility via three possibilities of coordination modes, i.e. monodentate, chelation bidentate, chelating–bridging tridentate. The pseudo-cyclic conformation of the acyclic EO5 ligand after the formation of monomeric $[Er(Pic)_2(EO5)](Pic)$ complex was observed in the inner-coordination sphere of $[Er(Pic)_2(EO5)]^+$. The flexible structure of the EO5 ligand and the Pic anions in the monomeric complex have an important role to control the inner-coordination sphere. The PL spectrum of this complex is composed of a broad band due to the emission of the aromatic organic ligands (Pic anion) and a shoulder peak originating from the 4f–4f emission transition of the Er(III) ion. Despite their broad luminescence behavior in the visible region, their luminescence properties in the near infrared region remain to be exploited.

Interesting future research would on the systematic investigation of the organic ligands efficient for the energy transfer to the Er(III) ion. Promising class of compounds are the aromatic carboxylic acids and the flexible organic compounds. Sensitizer materials doped on to the Er(III) complexes is also interesting. For the sensitizers, there is the possibility of sensitizing the luminescence of a lanthanide ion via another metal ion, being a lanthanide or a transition-metal ion. The multiply doped metal ions would be able to offer the opportunity of designing materials with a tunable emission color, depending on the concentration and ratio of the metal ions, the excitation wavelength, and the temperature. The energy transfer process in the complexes could be optimized with maximize the overlap between the emission spectrum of donor atom and absorption spectrum of acceptor atom. Furthermore, research on searching the Er(III) complexes that give designs of new complexes to improve the luminescence properties, thus they could become more and more in favor for luminescent-based applications.

Supplementary Material

CCDC 693440 and 247730 supplementary crystallographic data for the $[Er_2(9\text{-AC})_6(DMF)_2(H_2O)_2]$ and $[Er(Pic)_2(EO5)](Pic)$ complexes, respectively. These data can be obtained free of charge from the Cambridge Crystallographic Data Center via www.ccdc.cam.ac.uk/data_request/cif.

Acknowledgments We thank to Universitas Indonesia for financial support by the research grant RUUI bidang Unggulan No. 2589/H2.R12/PPM.00.01 Sumber Pendanaan/2010.

References

1. Saleh MI, Kusrini E, Adnan R, Rahman IA, Saad B, Usman A, Fun HK, Yamin BM (2005) J Chem Crystallogr 35:469
2. Saleh MI, Kusrini E, Saad B, Adnan R, Mohamed AS, Yamin BM (2007) J Lumin 126:871
3. Saleh MI, Kusrini E, Adnan R, Saad B, Yamin BM, Fun HK (2007) J Mol Struct 837:169
4. Saleh MI, Kusrini E, Saad B, Fun HK, Yamin BM (2009) J Alloys Compd 474:428
5. Kusrini E, Saleh MI, Lecomte C (2009) Spectrochim Acta Part A 74:120
6. Saleh MI, Kusrini E, Mohd Sarjidan MA, Abd. Majid WH (2010) Spectrochim Acta Part A, in press
7. Kusrini E, Saleh MI, Adnan R, Za'aba NK, Abd. Majid WH (2010) J Lumin, Accepted
8. Kusrini E (2010) Inorg Chim Acta 363:2533
9. Polman A (1997) J Appl Phys 82:1
10. Slooff LH, van Blaaderen A, Polman A, Hebbink GA, Klink SI, Van Veggel FCJM, Reinhoudt DN, Hofstraat JW (2002) J Appl Phys 91:3955
11. Destri S, Pasini M, Porzio W, Rizzo F, Dellepiane G, Ottonelli M, Musso G, Meinardid F, Veltri L (2007) J Lumin 127:601
12. Blasse J (1979) In: Gschneidner KA, Eyring L (eds) Handbook on the physics and chemistry of rare earths, vol 4. Elsevier, Amsterdam
13. Sanchez C, Lebeau B, Chaput F, Boilot JP (2003) Adv Mater 15:1969
14. Sanchez C, Julian B, Belleville P, Popall M (2005) J Mater Chem 15:3559
15. Liu SX, Liu WS, Tan MY, Ytl KB (1997) Polyhedron 16:1491
16. Kusrini E, Saleh MI (2009) Inorg Chim Acta 362:4025
17. Kusrini E, Adnan R, Saleh MI, Yan LK, Fun HK (2009) Spectrochim Acta Part A 72:884
18. Thiakou KA, Nastopoulos V, Terzis A, Raptopoulou CP, Perlepes SP (2006) Polyhedron 25:539
19. Wei PR, Wu DD, Zhou ZY, Li SL, Mak TCW (1997) Polyhedron 16:749
20. Aparna K, Krishnamurthy SS, Nethaji M, Balaram P (1997) Polyhedron 16:507
21. Wang RY, Zhao JJ, Jin TZ, Xu GX, Zhou ZY, Zhou XG (1998) Polyhedron 17:43
22. Deacon GB, Forsyth M, Junk PC, Leary SG, Moxey GJ (2006) Polyhedron 25:379
23. Carlos LD, Malta OL, Albuquerque RQ (2005) Chem Phys Lett 415:238
24. Garcia D, Faucher M (1985) J Chem Phys 82:5554
25. Bünzli J-CG, André N, Elhabiri M, Muller G, Piguet C (2000) J Alloys Compd 303–304:66
26. Hasegawa Y, Wada Y, Yanagida SJ (2004) Photochem Photobiol C: Photochem Rev 5:183
27. Yang C, Sun Z-F, Liu L, Zhang L-QJ (2008) Mater Sci 43:1681
28. Bruker (2000) SADABS (version 2.01), SMART (V5.603) and SAINT (V 6.36a). Bruker AXS Inc., Madison

29. Sheldrick GM (1997) SHELXTL V5.1. Bruker AXS Inc., Madison
30. Spek AL (2003) J Appl Crystallogr 36:7
31. Liu C-S, Chen P-Q, Chang Z, Wang J-J, Yan L-F, Sun H-W, Bu X-H, Lin Z, Li Z-M, Batten SR (2008) Inorg Chem Commun 11:159
32. Fitzgerald LJ, Gerkin RE (1997) Acta Crystallogr C53:71
33. Oisher U, Feinberg F, Frolow F, Shohum G (1996) Pure Appl Chem 68:1195
34. Saleh MI, Kusrini E, Fun HK, Yamin BM (2008) J Organomet Chem 693:2561
35. Sabbatini N, Guardigli M, Lehn J-M (1993) Coord Chem Rev 123:201
36. Fujii T, Nagai T, Uehara A, Yamana H (2007) J Alloys Compd 441:L10
37. Rogers RD, Zhang J, Bauer CB (1997) J Alloys Compd 249:41
38. Liu HQ, Cheung TC, Che CM (1996) Chem Commun 1039
39. Guo YL, Dou W, Wang YW, Liu WS, Wang DQ (2007) Polyhedron 26:1699
40. Park OH, Pinot J, Bae BSJ (2004) Sol–Gel Sci Technol 32:273
41. Filipescu N, Sager WF, Serafin FAJ (1964) Phys Chem 68:3324
42. Bünzli J-CG, Chauvin A-S, Kim HK, Deiters E, Eliseeva SV (2010) Coord Chem Rev 254:2623